

# DESIGN AND EXPERIMENT OF THRESHING AND SEPARATING DEVICE OF CORN GRAIN HARVESTER

## 玉米籽粒收获机脱粒分离装置设计与试验研究

Zhicai SONG, Peisong DIAO\*), Huanxiao PANG, Dianbao ZHAO, Hequan MIAO, Xiaowei LI, Duozen YANG <sup>1</sup>

School of Agricultural and Food Science, Shandong University of Technology, Zibo/China

Tel: +86-13864306142; E-mail: dps2003@163.com

Corresponding author: Diao Peisong

DOI: <https://doi.org/10.35633/inmateh-66-18>

**Keywords:** corn; threshing and separation device; multifactor test

### ABSTRACT

In order to find out the influence rule of threshing system parameters on threshing effect and the optimal parameter combination, the cylinder-concave clearance adjustment device is realized by "Front and back two hydraulic cylinders + Slide rail", the deflector angle adjustment device is realized by "Hydraulic cylinder driving hinge rotation" and the threshing separation device inclination angle adjustment device is realized by "Front adjustable double head pull rod". Multi-objective optimization test was carried out. The experimental results showed that the significant order of the influence of various factors on the grain breakage rate was rotational speed of roller, threshing separation device inclination angle, feeding rate, deflector angle and cylinder-concave clearance. The order of significance of the influence on uncleaned material rate was rotational speed of roller, cylinder-concave clearance, deflector angle, threshing device angle and feeding rate. According to the multi-objective parameter optimization analysis, the optimal operation parameter combination of corn threshing was determined. Under this parameter combination condition, model verification test and field optimization test were carried out. Compared with the field test value after parameter optimization, the grain breakage rate decreased from 4.018% to 3.462%, and the uncleaned material rate decreased from 0.292% to 0.218%.

### 摘要

为寻求脱粒系统参数对脱粒效果的影响规律及最优参数组合,设计了前后两油缸加滑轨的脱粒间隙调节装置、油缸伸缩带动合页转动的导流板角度调节装置以及前端可调节双头拉杆的脱粒分离装置倾角调节装置。进行多目标优化试验。试验结果表明:各因素对籽粒破碎率影响的显著性大小顺序为滚筒转速、脱粒分离装置倾角、喂入量、导流板角度及脱粒间隙;对未脱净率影响的显著性大小顺序为滚筒转速、脱粒间隙、导流板角度、脱粒分离装置倾角及喂入量。通过多目标参数优化分析,确定装置进行玉米脱粒的最优作业参数组合,在该参数组合条件下进行了模型验证试验以及田间优化试验,参数优化前与参数优化后田间试验值相比,籽粒破碎率由4.018%降为3.462%,未脱净率由0.292%降为0.218%。

### INTRODUCTION

The corn grain harvester can complete crop harvesting, threshing, separation and other processes at once (Chen et al., 2012; Chen et al., 2018). The threshing and separating device is the core component of the corn grain harvester, which directly affects the grain breakage rate and the uncleaned material rate during corn harvesting (Miu et al., 2019; Miu et al., 1997; Kutzbach et al., 2008). For the threshing and separation device, scholars have done numerous researches (Cui et al., 2019; Geng et al., 2019; Yang et al., 2019; Chen et al., 2020, Cujbescu D. et al, 2021, Wang S.S., 2021). Although scholars at home and abroad have done a lot of research on the axial flow threshing and separating device, there are still problems of uncleaned material threshing and high crushing rate during harvesting, and when the feeding rate fluctuates, it is easy to block the drum. Therefore, in-depth research is needed for the above issues.

<sup>1</sup> Zhicai Song, Stud.; Peisong Diao, Prof. Ph.D.; Huanxiao Pang, Stud.; Dianbao Zhao, Stud.; Hequan Miao, Stud.; Xiaowei Li, Stud.; Duozen Yang, Stud.

This paper is designed to study the rotational speed of roller, feeding rate, threshing separation device inclination, the deflector angle and the cylinder-concave clearance on the operation effect of the device, using the quadratic rotation orthogonal combination design method to carry out multi-objective optimization experiments (Qian et al., 2017; Liao et al., 2019; Teng et al., 2020; Omid et al., 2010), establish the correlation model of each operation index and each influencing factor, analyze the influence of each influencing factor on the operation index laws, and obtain the best combination of operating parameters of the device, in order to provide a reference for improving the operating performance of the longitudinal axial flow threshing device.

## MATERIALS AND METHODS

### Overall structure and working principle

The overall structure of the longitudinal axial flow corn flexible threshing and separating device is shown in Figure 1. It is composed of a feeding device, a frame, an inclination adjustment device, an upper cover device, a conical threshing drum, a cylinder-concave clearance adjustment device, a control device and a grain collection box. Among them, the feeding device conveys the corn ears from the bottom to the corn threshing and separating device, which can achieve the effect of uniform feeding. The conical threshing drum is equipped with spirally distributed threshing elements. In order to coordinate with the axial conveying of the ears by the threshing elements, there is a uniformly adjustable spiral baffle in the upper cover. The conical flexible threshing drum and the shell are installed above the frame. The threshing and separating device installed in cooperation with the frame and the front end of the threshing and separating device realizes the adjustment of the inclination angle of the threshing and separating device. The crushing and separation effects of grains in different areas are observed.

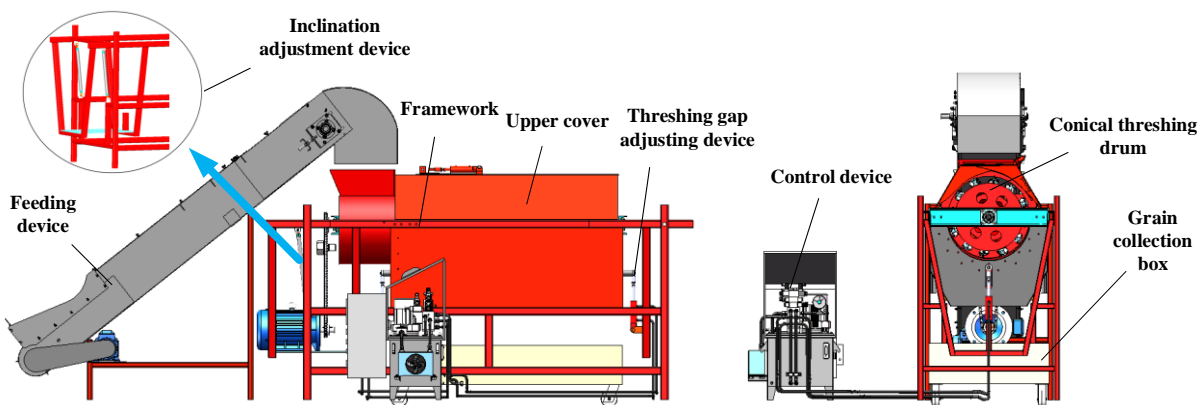


Fig. 1 - Overall structure of longitudinal axial flow threshing and separation test rig

### Cylinder-concave clearance adjustment

The cylinder-concave clearance mainly refers to the gap between the threshing drum and the concave screen. The cylinder-concave clearance adjustment device is mainly composed of hydraulic cylinder, support round tube, slide, side panel, inclined board, concave screen. As shown in Figure 3, the cylinder-concave clearance is adjusted by the expansion and contraction of the cylinders on both sides, and the four slide rails on both sides ensure the vertical movement of the segmented concave screen. The side panels on both sides prevent grains from falling from both sides.

Since the designed threshing drum is a cone-shaped threshing drum, the designed cylinder-concave clearance  $\delta$  is the average gap between the front and rear ends, which can be obtained as follows:

$$\delta = \frac{\delta_1 + \delta_2}{2} \quad (1)$$

where:

$\delta$  is the defined cylinder-concave clearance, [mm];

$\delta_1$  is the distance between the rear end of the drum and the concave screen, [mm];

$\delta_2$  is the distance between the front end of the drum and the concave screen, [mm].

The two hydraulic cylinders at the front and rear are the power unit of the concave screen. The designed oil circuit is shown in Figure 4. The adjustment range of the recessed plate gap is 35 mm~60 mm. The speed control valve plays the role of speed control, and the range is 0 mm/s~10 mm/s.

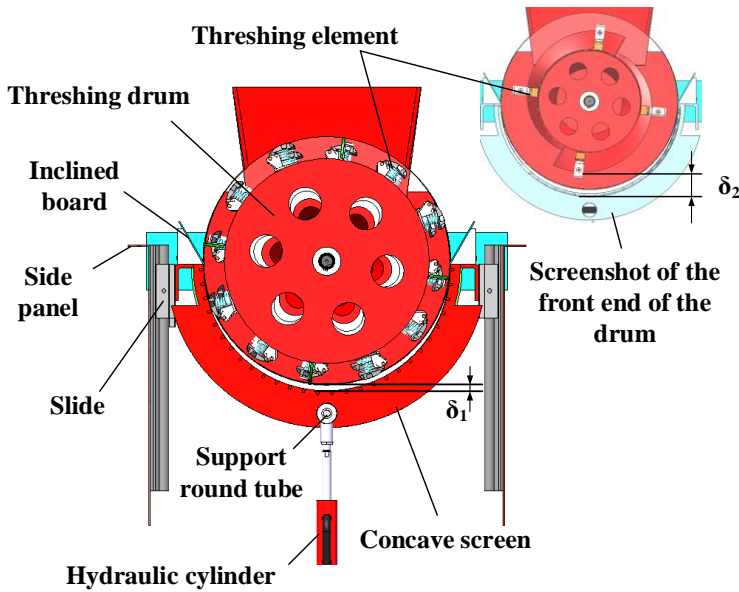


Fig. 3 - Cylinder-concave clearance adjustment design  
Angle adjustment of the deflectors

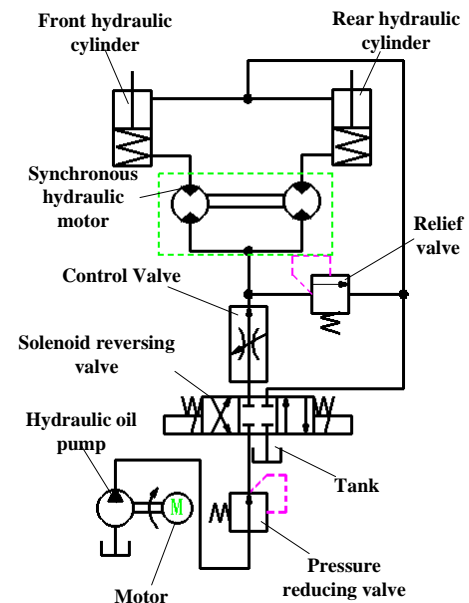
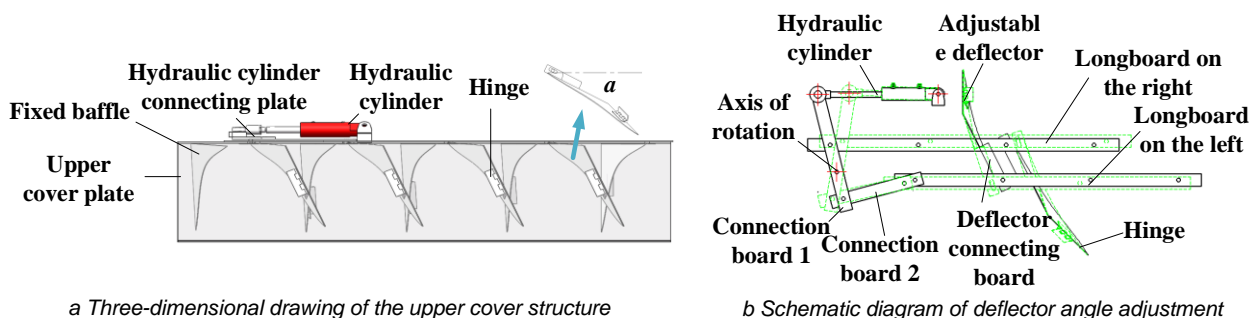


Fig. 4 - Cylinder-concave clearance regulation oil circuit

The upper cover in the threshing and separating device is located above the drum and forms a complete threshing chamber with the concave screen. The inner surface of the top cover is designed with orderly arranged deflectors, and the inclination angle of the deflectors is adjusted by hydraulic cylinders, thereby changing the staying time of the corn ears in the threshing chamber.

The structure of the upper cover is mainly composed of upper cover plate, deflector, hydraulic cylinder, connecting plate, etc., as shown in Figure 5. The angle of the deflector is adjusted by the expansion and contraction of the hydraulic cylinder, as shown in Figure 5.

When the angle of the deflector is too large, the time of the corn ears staying in the threshing and separating device becomes longer, which increases the threshing time of the corn ears, which is beneficial to improve the removal rate, but it is easy to cause the retention, accumulation or blockage of the ears. If the time is too long, the rate of kernel breakage will increase significantly, and the degree of breakage of corn cobs and bracts will also increase, which increases the load of subsequent cleaning and significantly increases the impurity rate. The angle  $\alpha$  of the deflector on the top cover is adjustable from 60° to 80°.



a Three-dimensional drawing of the upper cover structure

b Schematic diagram of deflector angle adjustment

Fig. 5 - Upper cover structure drawing

**Angle adjustment of threshing and separating device**

Since the working inclination angle of the threshing and separating device affects the subsequent transportation efficiency of corn ears, the working inclination angle of the threshing and separating device is an important factor affecting the efficiency of threshing and separating. It adopts an adjustable double-ended tie rod structure, as shown in Figure 6.

Adjust the height of the front end of the longitudinal axial flow threshing and separating device through the knob of the double-headed reverse screw bolt to realize the inclination adjustment. The adjustable height of the double-headed pull rod is 0 mm~300 mm, which can realize the change adjustment of the inclination angle of the threshing and separating device from 0° ~6°.

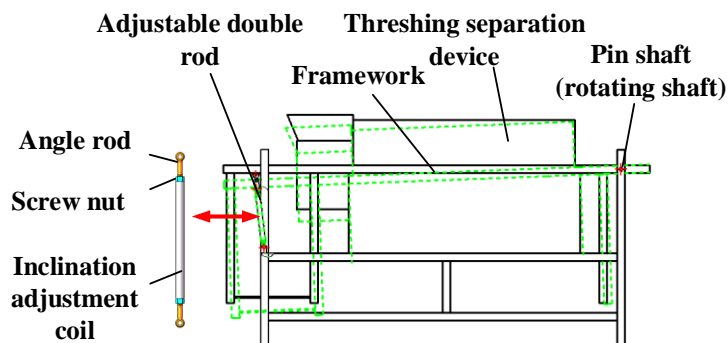


Fig. 6 - Angle adjustment mechanism

**RESULTS**

**Test purpose and materials**

In order to explore the influence of various factors in the threshing system on the grain crushing rate and unremoved material rate and the best parameter combination, the corn threshing parameter optimization test was carried out in the Agricultural Machinery Equipment Laboratory of Shandong University of Technology from October 12 to 18, 2021. The test site is shown in Figure 7. The test material is "Liyuan 296". Before the test, the basic characteristic parameters of corn ears are measured randomly using vernier calipers and 101-OBS electric heating blast drying oven.

The basic characteristic parameter values of corn ears are shown in Table 1.

**Table 1**

Material characteristics of corn	
Parameter	Numerical value
Natural plant height	279.7cm
Ear height	104.8cm
Average number of grains per ear	474.1
Average ear length	17.2cm
Average diameter of big end	52.34cm
Average diameter of small end	37.87cm
Average corn kernel moisture content	30.16%



a. Test site



b. Unbroken kernel



c. Broken kernels

Fig. 7 - Test scene photos

**Test results and analysis**

According to the Box-Behnken central combination design theory, response surface tests were carried out on the rotational speed of roller *A*, feeding rate *B*, cylinder-concave clearance *C*, deflector angle *D*, and threshing separation device inclination angle *E* with the grain breakage rate *Y*<sub>1</sub> and the uncleaned material rate *Y*<sub>2</sub> as response values (Teng et al., 2012; Chen et al., 2018). The optimization test plan and results of the threshing operation parameters of corn ears are shown in Table 2.

**Table 2**

Experimental design scheme and results							
No.	<i>A</i> <sup>[a]</sup>	<i>B</i> <sup>[b]</sup>	<i>C</i> <sup>[c]</sup>	<i>D</i> <sup>[d]</sup>	<i>E</i> <sup>[e]</sup>	<i>Y</i> <sub>1</sub> <sup>[f]</sup>	<i>Y</i> <sub>2</sub> <sup>[g]</sup>
1	500	7	5	70	50	5.3	0.32
2	450	7	5	70	45	3.3	0.23
3	400	7	5	80	45	3.08	0.58
4	450	7	5	70	45	3.54	0.25
5	450	7	4	80	45	4.64	0.64

No.	A <sup>[a]</sup>	B <sup>[b]</sup>	C <sup>[c]</sup>	D <sup>[d]</sup>	E <sup>[e]</sup>	Y <sub>1</sub> <sup>[f]</sup>	Y <sub>2</sub> <sup>[g]</sup>
6	450	7	5	60	50	4.56	0.34
7	400	7	4	70	45	4.13	0.72
8	500	7	5	70	40	3.86	0.18
9	500	7	4	70	45	5.98	0.43
10	400	6	5	70	45	3.13	0.44
11	450	8	5	70	50	4.41	0.38
12	500	8	5	70	45	5.32	0.26
13	400	7	5	60	45	3.64	0.41
14	450	7	5	70	45	3.14	0.23
15	450	7	5	80	50	4.12	0.51
16	450	6	4	70	45	4.32	0.48
17	450	7	6	70	40	2.85	0.18
18	450	7	6	80	45	3.07	0.4
19	500	7	5	80	45	4.26	0.32
20	450	8	4	70	45	4.03	0.52
21	450	7	5	70	45	3.26	0.21
22	400	7	6	70	45	3.42	0.42
23	400	7	5	70	50	3.43	0.56
24	450	7	4	70	50	5.01	0.58
25	450	8	5	80	45	3.28	0.42
26	450	7	5	70	45	3.08	0.23
27	450	7	4	70	40	4.41	0.41
28	500	7	6	70	45	4.04	0.25
29	450	7	5	70	45	3.43	0.25
30	450	6	5	70	40	2.45	0.15
31	400	7	5	70	40	3.23	0.34
32	450	6	5	80	45	2.54	0.4
33	450	8	5	70	40	3.66	0.19
34	450	7	4	60	45	4.99	0.47
35	450	6	5	70	50	3.07	0.34
36	450	6	6	70	45	2.49	0.25
37	450	7	5	80	40	3.28	0.31
38	450	6	5	60	45	3.08	0.21
39	450	8	6	70	45	3.57	0.24
40	500	6	5	70	45	2.42	0.16
41	450	7	6	70	50	3.42	0.33
42	450	8	5	60	45	4.45	0.26
43	400	8	5	70	45	3.38	0.46
44	450	7	5	60	40	3.62	0.18
45	450	7	6	60	45	3.42	0.24
46	500	7	5	60	45	4.92	0.22

<sup>[a]</sup> Rotational speed of roller / r/min ; <sup>[b]</sup> Feeding rate / kg/s ; <sup>[c]</sup> Threshing separation device inclination angle/°; <sup>[d]</sup> Deflector angle/° <sup>[e]</sup> Cylinder-concave clearance / mm; <sup>[f]</sup> The grain breakage rate/%; <sup>[g]</sup> The uncleaned material rate/%.

According to the test results in the table, Design-Expert software is used to statistically analyze the test data. The regression equation of grain damage rate  $Y_1$  to the rotational speed of roller  $A$ , the feed rate  $B$ , threshing separation device inclination angle  $C$ , the deflector angle  $D$ , and cylinder-concave clearance  $E$  was established, and the significance of experimental factors was analyzed.

Multivariate regression fitting of the experimental data, eliminating the insignificance in the model, and obtaining the regression equation of the influence of the grain breakage rate  $Y_1$  and the uncleaned material rate  $Y_2$ .

$$Y_1 = 3.29 + 0.54A + 0.54B - 0.7C - 0.28D + 0.37E + 0.66AB - 0.31AC + 0.31AE + 0.34BC \tag{1}$$

$$+ 0.48A^2 - 0.18B^2 + 0.5C^2 + 0.26D^2 + 0.24E^2$$

$$Y_2 = 0.21 - 0.11A + 0.014B + 0.086C + 0.089D - 0.11E + 0.03AB - 0.028AC - 0.03AD + 0.027AE$$

$$+ 0.099A^2 + 0.017B^2 + 0.033C^2 + 0.093D^2 + 0.11E^2 \tag{2}$$

The grain breakage rate  $Y_1$  and the uncleaned material rate  $Y_2$  variance analysis table is shown in Table 3.

Table 3

Variance analysis of regression equation of grain breakage rate and uncleaned material rate

Grain breakage rate					Uncleaned material rate				
Source	Sum of squares	D <sub>f</sub>	F-value	P-value	Source	Sum of squares	D <sub>f</sub>	F-value	P-value
Model	28.62	14	34.39	< 0.01	Model	0.91	14	108.66	< 0.01
A	4.69	1	78.84	< 0.01	A	0.19	1	323.10	< 0.01
B	4.62	1	77.75	< 0.01	B	3.025×10-3	1	5.05	0.0319

**Table 3**  
(continuation)

Grain breakage rate					Uncleaned material rate				
Source	Sum of squares	Df	F-value	P-value	Source	Sum of squares	Df	F-value	P-value
<b>C</b>	7.88	1	132.58	< 0.01	<b>C</b>	0.12	1	195.77	< 0.01
<b>D</b>	1.22	1	20.44	< 0.01	<b>D</b>	0.13	1	213.30	< 0.01
<b>E</b>	2.22	1	37.34	< 0.01	<b>E</b>	0.21	1	345.51	< 0.01
<b>AB</b>	1.76	1	29.53	< 0.01	<b>AB</b>	3.600×10-3	1	6.01	0.0201
<b>AC</b>	0.38	1	6.36	0.0170	<b>AC</b>	3.025×10-3	1	5.05	0.0319
<b>AE</b>	0.38	1	6.47	0.0162	<b>AD</b>	3.600×10-3	1	6.01	0.0201
<b>BC</b>	0.47	1	7.89	< 0.01	<b>AE</b>	3.025×10-3	1	5.05	0.0319
<b>A<sup>2</sup></b>	1.98	1	33.35	< 0.01	<b>A<sup>2</sup></b>	0.085	1	142.63	< 0.01
<b>B<sup>2</sup></b>	0.30	1	5.02	0.0323	<b>B<sup>2</sup></b>	2.609×10-3	1	4.35	0.0452
<b>C<sup>2</sup></b>	2.16	1	36.33	< 0.01	<b>C<sup>2</sup></b>	9.576×10-3	1	15.98	< 0.01
<b>D<sup>2</sup></b>	0.59	1	9.99	< 0.01	<b>D<sup>2</sup></b>	0.076	1	126.31	< 0.01
<b>E<sup>2</sup></b>	0.50	1	8.34	< 0.01	<b>E<sup>2</sup></b>	0.18	1	294.90	< 0.01
<b>Residual</b>	1.84	31			<b>Residual</b>	0.019	31		
<b>Lack of fit</b>	1.69	26	2.18	0.1975	<b>Lack of fit</b>	0.016	26	1.03	0.5487
<b>Error</b>	0.15	5			<b>Error</b>	2.933×10-3	5		
<b>Sum</b>	30.47	45			<b>Sum</b>	0.93	45		

Note: P<0.01 (very significant); 0.01≤P<0.05 (significant); P≥0.05 (not significant).

The contribution value *K* can reflect the degree of influence of a single factor on the established model. The larger the value of *K*, the greater the degree of influence of the factor on the model. The calculation methods are shown in Eq.3 and Eq.4.

$$K_i = \delta_i + \frac{1}{4} \sum \delta_{ij} + \delta_{i,2} \tag{3}$$

$$\delta = \begin{cases} 0, & F \leq 1 \\ 1 - \frac{1}{F}, & F > 1 \end{cases} \tag{4}$$

where *i* is the assessment value, *i, j* = A, B, C, D, E, and *i* ≠ *j*.

According to formula (2) and formula (3), the contribution values of rotational speed of roller, feed rate, inclination angle of threshing separation device, deflector angle and cylinder-concave clearance to the crushing rate are calculated to be 2.621, 2.248, 2.394, 1.851 and 2.065, respectively. Therefore, the significant order of the influence of various factors on the crushing rate is the rotational speed of roller, the inclination angle of the threshing and separating device, the feeding rate, the deflector angle and the cylinder-concave clearance. The contribution of rotational speed of roller, feed rate, inclination angle of the threshing and separating device, deflector angle and cylinder-concave clearance to the uncleaned material rate are calculated to be 2.856, 1.780, 2.133, 2.196 and 2.243 respectively. Therefore, the significant order of the influence of various factors on the uncleaned material rate is the rotational speed of roller, the cylinder-concave clearance, deflector angle, the inclination angle of the threshing and separating device and the feeding rate.

When studying actual problems, it is usually necessary to consider the influence of the interaction of two factors on the test results. Respectively set C=D=E=0, B=D=E=0, B=C=D=0, A=D=E=0, and get the interaction factors AB, AC, AE, BC to the grain breakage rate *Y*<sub>1</sub>. The law of influence is shown in Figure 8. Respectively set C=D=E=0, B=D=E=0, B=C=E=0, B=C=D=0, and get the interaction factors AB, AC, AD, AE on the uncleaned material rate *Y*<sub>2</sub>. The law of influence is shown in Figure 9.

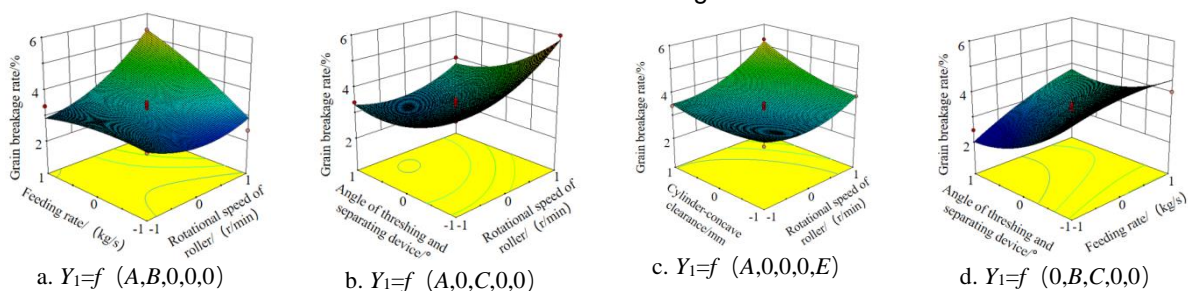


**Fig. 8 - Effects of interaction of various factors on the grain breakage rate**

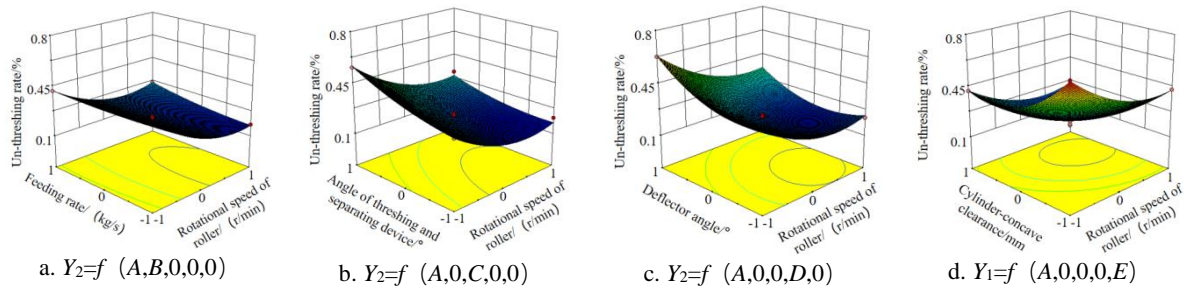


Fig. 9 - The influence of the interaction of various factors on the uncleaned material rate

It can be seen from Figure 8a that in the interaction of the rotational speed of roller A and the feeding rate B on the grain breakage rate  $Y_1$ , the rotational speed of roller has a greater influence on the interaction. When the rotational speed of roller is 400 r/min and the feeding rate is 6 kg/s, the grain breakage rate is the smallest. It can be seen from Figure 8b that in the interaction of the rotational speed of roller A and the inclination angle of the threshing and separating device C on the grain breakage rate  $Y_1$ , the rotational speed of roller has a greater influence on the interaction. When the rotational speed of roller is 400 r/min and the inclination angle of the threshing and separating device is 6°, the grain breakage rate is the smallest. It can be seen from Figure 8c that in the interaction between the rotational speed of roller A and the cylinder-concave clearance E on the grain breakage rate  $Y_1$ , the rotational speed of roller has a greater impact on the interaction. When the rotational speed of roller is 400 r/min and the cylinder-concave clearance is 40 mm, the grain breakage rate is the smallest. It can be seen from Figure 8d that in the interaction between the feeding rate B and the inclination angle of the threshing and separating device C on the grain breakage rate  $Y_1$ , the inclination angle of the threshing and separating device has a greater influence on the interaction. When the inclination angle of the threshing and separating device is 6°, the grain breakage rate is the smallest.

It can be seen from Figure 9a that in the interaction of the rotational speed of roller A and the feeding rate B on the uncleaned material rate  $Y_2$ , the rotational speed of roller has a greater influence on the interaction. When the rotational speed of roller is 500 r/min and the feeding rate is 6 kg/s, the uncleaned material rate is the smallest. It can be seen from Figure 9b that in the interaction of the rotational speed of roller A and the inclination angle of the threshing and separating device C on the uncleaned material rate  $Y_2$ , the rotational speed of roller has a greater influence on the interaction. When the rotational speed of roller is 500 r/min and the inclination angle of the threshing and separating device is 6°, the uncleaned material rate is the smallest. It can be seen from Figure 9c that in the interaction of the rotational speed of roller A and the deflector angle D on the uncleaned material rate  $Y_2$ , the rotational speed of roller has a greater influence on the interaction. When the rotational speed of roller is 500 r/min and the deflector angle is 40 mm, the uncleaned material rate is the smallest. It can be seen from Figure 9d that in the interaction between the rotational speed of roller A and the cylinder-concave clearance E on the uncleaned material rate  $Y_2$ , the cylinder-concave clearance has a greater impact on the interaction. When the cylinder-concave clearance is 45 mm and the rotational speed of roller is 450 r/min, the uncleaned material rate is the smallest.

**Parameter optimization and experimental verification**

Use the optimization module in Design-expert to determine the optimal combination of parameters, select test indicators; the range of conditions for test factors is shown in Table 4.

Table 4

Name	Factors limiting condition					$Y_1$	$Y_2$
	A	B	C	D	E		
Target range	in range	in range	in range	in range	in range	minimum	minimum
Lower limit	400	6	4	60	40	2.42	0.16
Upper limit	500	8	6	80	50	5.98	0.71

Note: The importance of kernel damage rate is set to "++++", and the importance of uncleaned material rate is set to "++++"

According to the optimization results, the rotational speed of roller is 476.7 r/min, the feed rate is 6 kg/s, the inclination angle of the threshing and separating device is 5.3°, the deflector angle is 68.2°, and the cylinder-concave clearance is 45.6 mm, the grain crushing rate is 2.420% and the uncleaned material rate is 0.178%.

In order to verify the accuracy of the prediction of each index model and the operating effect of the whole machine under the optimal parameter combination of the threshing system, the model prediction test was first carried out in the Agricultural Machinery Equipment Laboratory of Shandong University of Technology. The corn material characteristics during the test were the same as those in Table 1. The parameters of the threshing system were the optimal parameter combination, and 5 sets of parallel experiments were carried out. The test results are shown in Table 5. Under the optimal parameter combination conditions, the model verification test has a grain breakage rate of 2.523% and an uncleaned material rate of 0.186%. The relative errors of each evaluation index and the predicted value of the model are 4.21% and 4.50% respectively, both less than 5%, and the parameter optimization results are reliable. Afterwards, field test verification was carried out in the experimental field of Fenghuang Town, Linzi, Shandong province, China as shown in Figure 10. The test materials and methods were the same as above. Five groups of parallel tests were designed before and after parameter optimization. The test results are shown in Table 8. Before parameter optimization, compared with the field test value after parameter optimization, the grain breakage rate decreased from 4.018% to 3.462%, and the uncleaned material rate decreased from 0.292% to 0.218%.

Table 5

Test results of optimized parameter		
Project	Grain breakage rate (%)	Uncleaned material rate (%)
Model prediction	2.421	0.178
Verification test value	2.523	0.186
Relative error	4.21	4.50
Field test value before parameter optimization	4.018	0.292
Field test value after parameter optimization	3.462	0.218

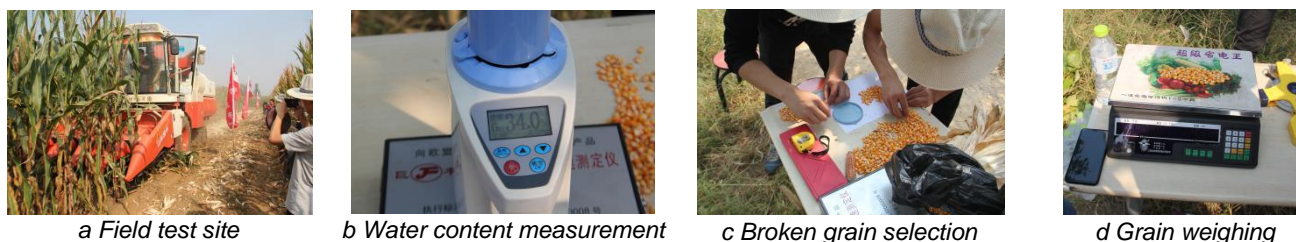


Fig. 10 - Photos of field test scenes

## CONCLUSIONS

(1) In order to seek the law and optimal influence of the parameters of the threshing system on the threshing effect combining parameters, a "Front and back two hydraulic cylinders + Slide rail" was designed, the deflector angle adjustment device was realized by "Hydraulic cylinder driving hinge rotation" and the threshing separation device inclination angle adjustment device was realized by "Front adjustable double head pull rod".

(2) Through multi-objective optimization experiments, a mathematical model of rotational speed of roller, feeding rate, the inclination angle of the threshing and separating device, deflector angle, cylinder-concave clearance, and the rates of corn threshing grain breakage and of uncleaned material were established. Through analysis, it can be seen that the significant order of the influence of various factors on the grain breakage rate model is the rotational speed of roller, the inclination angle of the threshing and separating device, the feeding rate, the deflector angle, and the cylinder-concave clearance. The significant order of the influence of various factors on the uncleaned material rate model is the rotation speed of roller, the cylinder-concave clearance, the deflector angle, the inclination angle of the threshing and separating device, and the feeding rate.

(3) A parameter optimization model of longitudinal axial flow threshing device was established, and the optimal parameters were as follows: roller rotational speed is 476.7 r/min, feeding rate is 6 kg/s, threshing separation device inclination angle is 5.3°, deflector angle is 68.2°, cylinder-concave clearance is 45.6 mm, the grain breakage rate is 2.420%, the uncleaned material rate is 0.178%. Verification test was conducted on this parameter combination, and the verification test results are as follows: The relative errors of each index and the predicted values were all less than 5%, which proved the correctness of the prediction model. The field experiment of parameter optimization was carried out, and the experimental results showed that the grain breakage rate and the uncleaned material rate after parameter optimization were lower than those before optimization.



## ACKNOWLEDGEMENT

The authors greatly appreciate the support from Shandong Province Agricultural Major Application Technology Innovation Project (SD2019NJ005); National key research and development programs (2018YFD0300606-04); and Shandong Province agricultural application technology innovation project (2019JZZY020615).

## REFERENCES

- [1] Chen M.Z., Xu G.F., Wei M.J., Song Z.C., Wang W.J., Diao P.S., Teng S.M., (2021), Longitudinal compressing and shearing properties of silage corn stalk in north China plain. *INMATEH – Agricultural Engineering*, vol. 65, no.3, pp. 47-56; DOI: <https://doi.org/10.35633/inmateh-65-05>
- [2] Chen Z., Hao F.P., Wang D., Su W.F., Cui J.W., (2012). Development of technology and equipment of corn harvester in China (中国玉米收获技术与装备发展研究). *Transactions of the Chinese Society for Agricultural Machinery*, 43 (12): 44-50.
- [3] Craessaerts G., Baerdemaeker J.D., (2010), Fuzzy control of the cleaning process on a combine harvester [J]. *Biosystems Engineering*, 2010, 106(2): 103-111.
- [4] Cui T., Fan C.L., Zhang D.X., Yang L., Li Y.B., Zhao H.H., (2019). Research progress of maize mechanized harvesting technology (玉米机械化收获技术研究进展分析). *Transactions of the Chinese Society for Agricultural Machinery*, 50 (12): 1 – 13.
- [5] Cujbescu D., Găgeanu I., Iosif A., (2021), Mathematical modeling of ear grain separation process depending on the length of the axial flow threshing apparatus. *INMATEH – Agricultural Engineering*, vol. 65, no.3, pp. 101-110. DOI: <https://doi.org/10.35633/inmateh-65-11>
- [6] Dai F., Song X.F., Zhao W.Y. et al, (2019), Motion simulation and test on threshed grains in tapered threshing and transmission device for plot wheat breeding based on CFD-DEM. *International Journal of Agricultural and Biological Engineering*, 12(1): 66-73.
- [7] Guan Z.H., Zhang Z., Jiang T., Li Y., Wu C.Y., Mu S.L., (2020), Development and test of speed control system for combine harvester threshing and cleaning device. *INMATEH – Agricultural Engineering*, vol. 61, no.2, pp. 305-314; DOI: <https://doi.org/10.35633/inmateh-61-33>
- [8] Kutzbach H.D., (2008), Modeling and simulation of grain threshing and separation in threshing units- Part I. *Computer and Electronics in Agriculture*, 2008, 60(1): 96-104.
- [9] Liao Q.X., Xu Y., Jiang Y.J., (2019). Design and experiment on combined tangential and throwing longitudinal axial flow threshing and separating device of rape combine harvester (油菜联合收获机切抛组合式纵轴流脱离装置设计与试验). *Transactions of the CSAM*, 2019; 50(7): 140–150.
- [10] Miu P.I., Beck F., Kutzbach H.D., (1997), Mathematical modeling of threshing and separating process in axial threshing units, *ASAE*, 1997: 97-106.
- [11] Omid M., Lashgair M., Mobli H., (2010). Design of fuzzy logic control system incorporating human expert knowledge for combine harvester. *Expert Systems with Applications*, 37(10): 7080-7085.
- [12] Qian Z.J., Jin C.Q. Zhang D.G., (2017), Multiple frictional impact dynamics of threshing process between flexible tooth and grain kernel. *Computers and Electronics in Agriculture*, 114:276-28.
- [13] Tang Z., Li Y.M., Xu L.Z., Li H.C., Pang J., (2012). Experiment and evaluating indicators of wheat threshing and separating on test-bed of longitudinal axial-threshing unit (切纵流联合收获机小麦脱粒分离性能评价与试验). *Transactions of the Chinese Society of Agricultural Engineering*, 28(3): 14-19.
- [14] Wang S.S., Chen P., Li J. T., Lu M.Q., (2021), Design and experimental study of flexible threshing unit for Chinese cabbage seeds. *INMATEH – Agricultural Engineering*, vol. 65, no. 3, pp. 333-344; DOI: <https://doi.org/10.35633/inmateh-65-35>.
- [15] Yang L.Q., Wang W.Z., Zang H.M., Li L.H., Wang M. M., Hou M.T., (2018), Improved design and bench test based on tangential flow-transverse axial flow threshing system (切流-横轴流玉米脱粒系统改进设计及台架试验). *Transactions of the Chinese Society of Agricultural Engineering*, 34(1): 35-43.
- [16] Zhu X.L., Chi R. J., Du Y.F., (2020), Experimental study on the key factors of low-loss threshing of high-moisture maize. *International Journal of Agricultural and Biological Engineering*, 2020, 13(5):23-31.